A PARADOX CONCERNING ION PERMEATION OF THE DELAYED RECTIFIER POTASSIUM ION CHANNEL IN SQUID GIANT AXONS

By JOHN R. CLAY

From the Laboratory of Biophysics, National Institute of Neurological Disorders and Stroke, National Institutes of Health, Bethesda, MD 20892 and the Marine Biology Laboratory, Woods Hole, MA 02453, USA

SUMMARY

1. The fully activated current–voltage relation ($I–V$) of the delayed rectifier potassium ion channel in squid giant axons has a non-linear dependence upon the driving force, $V-E_K$, as I have previously demonstrated, where V is membrane potential and E_K is the equilibrium potential for potassium ions.

2. The non-linearity of the $I–V$ relation and its dependence upon external potassium ion concentration are both well described, phenomenologically, by the Goldman–Hodgkin–Katz (GHK) flux equation, as I have also previously demonstrated. As illustrated below, this result can be modelled using the Eyring rate theory of single-file diffusion of ions through a channel in the low-occupancy limit of the theory.

3. The GHK equation analysis and the low-occupancy limit of the Eyring rate theory are both consistent with the independence principle for movement of ions through the channel, which is at odds with tracer flux ratio results from the delayed rectifier, published elsewhere. Those results suggest that the channel is multiply occupied by two, or perhaps three, ions.

4. The resolution of this paradox is provided by a triple-binding site, multiple-occupancy model in which only one vacancy, at most, is allowed in the channel. This model predicts current–voltage relations which are consistent with the data (and with the phenomenological prediction of the GHK flux equation). The model is also consistent, approximately, with the tracer flux ratio results.

INTRODUCTION

The delayed rectifier potassium ion channel in squid giant axons is known to be multiply occupied by potassium ions, based on the tracer flux ratio results of Begenisich & DeWeer (1980), and earlier results from similar experiments on cuttlefish axons by Hodgkin & Keynes (1955). These results strongly suggest that potassium ions do not move independently of one another as they pass through the channel. Rather, they appear to diffuse in single file along some number of negatively charged binding sites in such a manner that two or three of the sites are, on average,

always occupied by an ion (Hille & Schwarz, 1978). The other principle measure of ion permeation is the net flux, i.e. the fully activated current–voltage relation, which for the delayed rectifier was originally believed to be a linear function of driving force, $V-E_K$, where V is the membrane potential and E_K is the equilibrium potential for potassium ions (Hodgkin & Huxley, 1952a). However, this relation was demonstrated several years ago (Clay & Shlesinger, 1983; Clay, 1984) to be a non-linear function of $V-E_K$, which is well described by the Goldman–Hodgkin–Katz flux equation (Goldman, 1943; Hodgkin & Katz, 1949). Inferences about multiple occupancy cannot be drawn from the net flux. Nevertheless, the tracer flux and the current–voltage relation results taken together are suggestive of a paradox, inasmuch as the Goldman–Hodgkin–Katz (GHK) relation is based on independent movement of ions across the membrane, in contrast to the tracer flux results which clearly demonstrate that the independence principle does not apply. The paradox is further amplified by the work of Vestergaard-Bogind, Stampe & Christophersen (1985) and Neyton & Miller (1988), who have shown that calcium-activated potassium channels are multiply occupied even with low potassium ion activity on both sides of the channel. This result is surprising, because the independence principle would appear to apply under these conditions. These observations recently prompted Schumaker & MacKinnon (1990) to reinvestigate the 'single vacancy' model for potassium channels originally proposed by Kohler & Heckmann (1979) in which a channel is presumed to be either fully saturated, or to have at most a single vacancy which transiently moves through the channel, in low ion activity conditions. As shown below, this model is consistent with both the current–voltage relations and the tracer flux ratio results from the delayed rectifier in squid giant axons.

METHODS

Experiments were performed on common North Atlantic squid (*Loligo pealei*). The animals were killed by decapitation. Electrophysiological recordings from the giant axons were carried out using standard axial wire voltage clamp and internal perfusion techniques that have been previously described (Clay & Shlesinger, 1983). The temperature in these experiments ranged between 7 and 10 °C. In any single experiment it was maintained at a constant temperature, to within 0·1 °C, by a negative feedback circuit connected to a Peltier device mounted in the experimental chamber. The intracellular perfusate for most of these experiments consisted of 250 mM-potassium glutamate, 25 mM-K_2HPO_4, and 400 mM-sucrose, pH = 7·2. The perfusate for the experiments described in Fig. 5, in which intracellular potassium was altered so that $[K^+]_i = [K^+]_o$, consisted of either 50, 150, 250, or 450 mM-potassium glutamate and 25 mM-K_2HPO_4, with sucrose, adjusted to maintain an osmolarity of 1000 mosm. The external solution consisted of 0, 10, 50, 100, 300, or 500 mM-KCl with 440, 430, 390, 340, 140, or 0 mM-NaCl, respectively. These solutions also contained 50 mM-$MgCl_2$, 10 mM-$CaCl_2$, and 10 mM-Tris-HCl (pH = 7·2) and 0·5 mM-TTX (tetrodotoxin, Sigma). Liquid junction potentials were < 3 mV. The results in Figs 3 and 6 were corrected for these offsets.

RESULTS

Procedure for measuring current–voltage relations

The relative voltage dependence and external potassium ion concentration $[K^+]_o$ dependence of the fully activated current–voltage relation of the delayed rectifier current (I_K) was obtained by partially activating the conductance with voltage clamp pre-pulses to voltage levels which were close to E_K. This approach minimizes

potassium ion accumulation/depletion in the extracellular space between the axolemma and the Schwann cell around the axon during the pre-pulse. These results were obtained with elevated levels of $[K^+]_o$ in the 50–500 mM range, which serves to depolarize E_K into the range of activation of I_K. An example of this type of
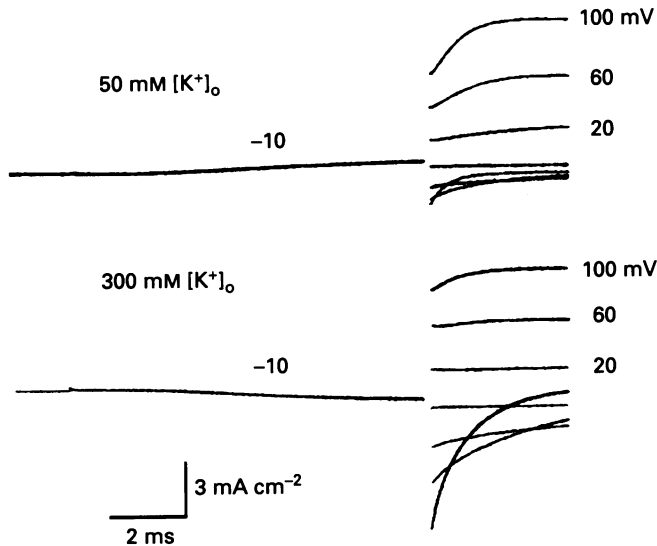

Fig. 1. Potassium current records from a squid giant axon, as described in the text, for 50 and 300 mM $[K^+]_o$. The holding potential was -80 mV. The pre-pulse level was -10 mV. The test levels were $+100$, 60, 20, -20, -60, -100, and -160 mV. Uncorrected records. (The leak current in this axon was virtually nil.) The first 150 μs of each test record has been deleted.

experiment is illustrated in Fig. 1 with $[K^+]_o = 50$ and 300 mM. A pre-pulse level of -10 mV was used as a compromise between the two values of E_K in this experiment ($E_K \sim -45$ and 0 mV for $[K^+]_o = 50$ and 300 mM, respectively). The holding level was -80 mV. The pre-pulse was followed by a test step to a voltage significantly different from E_K, followed by a return of the membrane potential to the holding level. A rest interval of 3 s was used between each two-pulse sequence. Superimposed sweeps of the membrane current for several test levels are shown in Fig. 1. The current–voltage relation was determined from the current immediately (150 μs) after the test step.

Effect of external potassium on gating?

One potential problem of the experiment described above is a possible effect of a change in $[K^+]_o$ on the degree of activation of I_K during the pre-pulse, a concern which is especially significant given the known effect of $[K^+]_o$ on the membrane current time constant at hyperpolarized levels (Swenson & Armstrong, 1981). This effect is also illustrated in Fig. 1. The deactivation, or 'tail', current time constant at -160 mV was increased by a factor of 2·4 in this experiment following a change in

$[K^+]_o$ from 50 to 300 mM. However, the activation time constant was unaltered, as illustrated in another experiment shown in Fig. 2, in which $[K^+]_o$ was changed from 50 to 500 mM. The current during a step to -20 mV is shown for both levels of $[K^+]_o$ with the 50 mM $[K^+]_o$ result scaled by a factor of -3. The scaled result and the
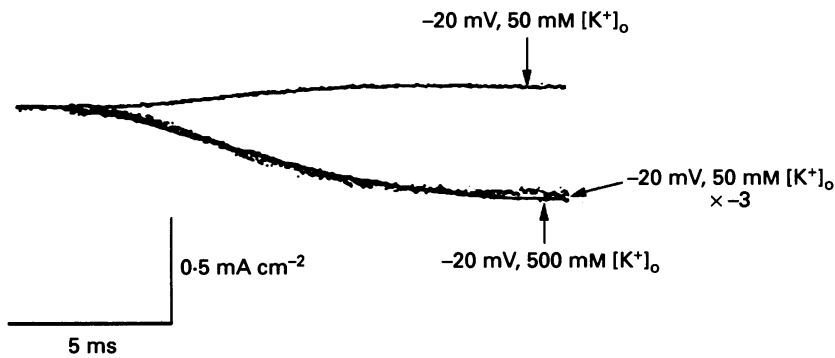

Fig. 2. Potassium current elicited by a step to -20 mV in 50 and 500 mM $[K^+]_o$. The 50 mM $[K^+]_o$ is also shown scaled by a factor of -3. Holding potential was -80 mV.

500 mM result essentially superimpose, which demonstrates that channel activation is unaltered by $[K^+]_o$, even when the direction of net current flow is reversed. Similar results are shown in Clay (1984).

Effect of $[K^+]_o$ on the current–voltage relation

The current–voltage relations from the experiment in Fig. 1 and from three other experiments are given in Fig. 3. These results show a lack of effect of a change in $[K^+]_o$ on outward current at strong depolarizations ($V > 80$ mV), which is consistent with intuition, inasmuch as $[K^+]_i$ was unchanged in these experiments. Conversely, the inward, or 'tail', current amplitude at strong hyperpolarizations was significantly increased by an increase in $[K^+]_o$, which is clearly evident, by eye, in Fig. 1. These results are well described by the Goldman–Hodgkin–Katz flux equation (hereafter referred to as the GHK equation) which is given by

$$\bar{I}_K = P_K F(FV/RT)\,([K^+]_i \exp\,(FV/RT) - [K^+]_o)/(\exp\,(FV/RT) - 1), \qquad (1)$$

where $\bar{I}_K$ refers to the fully activated current of the delayed rectifier, F is the Faraday constant, R is the gas constant, T is the absolute temperature, and P_K is the permeability of the membrane to potassium ions. The quantity $RT/F = 24.1$ mV for $T = 8\ ^\circ$C, which is representative of the temperature used in these experiments (Methods). For the sake of compactness, FV/RT is represented by V' in subsequent equations. Equation (1) provides a good, phenomenological fit to the data in Fig. 3 (lines labelled a). An alternative model for ion permeation across nerve membranes is provided by single-file diffusion of ions along some number of negatively charged sites separated by barriers to movement of ions within the channel pore, a process which can be described by the Eyring rate theory (Glasstone, Laidler & Eyring, 1941; Hille & Schwarz, 1978). This model gives an expression which is similar to that of the

GHK equation for the barrier profile shown in Fig. 4 A, in which the barriers are symmetrical and identical, and one ion, at most, is allowed to reside within the channel. The prediction of the model for these conditions is

$$J_{\mathrm{K}} \cong (1 - \exp(-V'/2m))([\mathrm{K}^+]_i \exp(V') - [\mathrm{K}^+]_o)/\exp(V') - 1), \qquad (2)$$
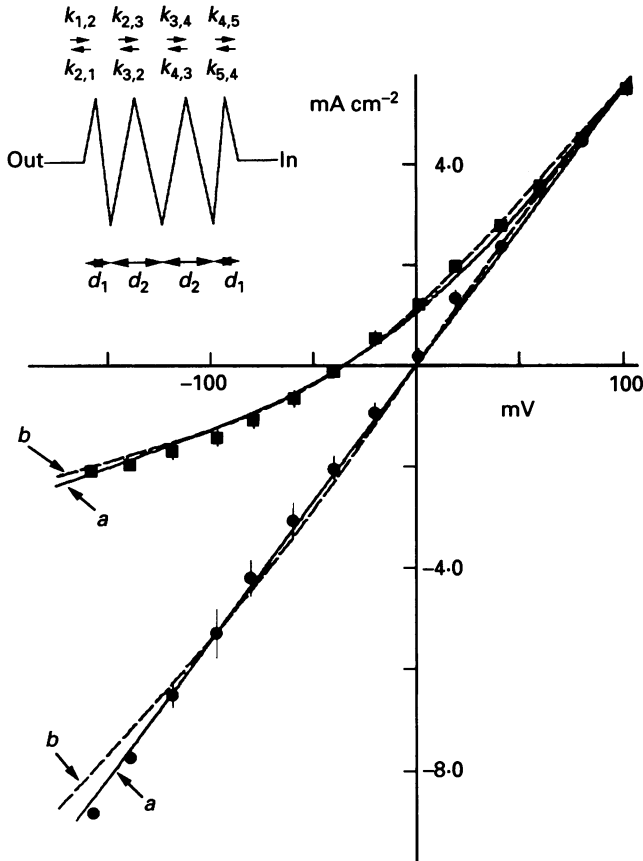
Fig. 3. Current–voltage relations from experiments as described in Fig. 1. (The currents were measured 150 μs after the test step in the voltage clamp protocol.) The vertical lines through some of the points refer to the standard deviation ($n = 4$). (The results for -137 and -157 mV correspond to a single experiment.) The lines labelled a are the best fit, by eye, to these results of the GHK equation (eqn (1) in the text). The permeability, P_{K} (same for both levels of $[\mathrm{K}^+]_o$), was adjusted so as to achieve the best fit to these results ($P_{\mathrm{K}} = 0.44 \times 10^{-4}$ cm s^{-1}). The dashed lines (labelled b) are the best fit to these results of the single occupancy model described in Fig. 4 A. This model is also illustrated in the inset ($d_1 = 0.08$; $d_2 = 0.17$). The various rate constants are defined in the Appendix. ■, 50 mM $[\mathrm{K}^+]_o$; ●, 300 mM $[\mathrm{K}^+]_o$.

where J_{K} is the potassium flux and m is the number of barriers (see Appendix). (Note that $m = n + 1$, where n is the number of binding sites within the channel.) In the limit $m \to \infty$, eqn (2) takes on the same voltage dependence as the GHK equation,

given that $1-\exp{(-V'/2m)} \cong (V'/2m)$ for large m. However, the channel probably contains only a relatively small number of binding sites, perhaps three ($n = 3$; $m = 4$) (Discussion). The prediction of eqn (2) for $m = 4$ (not shown) does not provide a good fit to the data in Fig. 3. A better fit can be obtained by adjusting the electrical
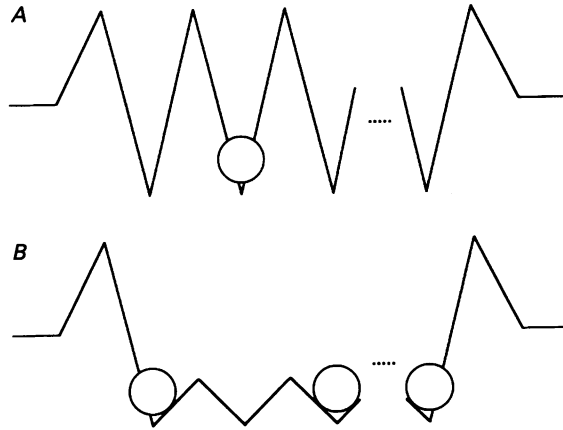

Fig. 4. Schematic representation of the single occupancy (A) and single vacancy (B) models. These diagrams refer to the free energy profile ($V = 0$) of a potassium ion within the channel for an arbitrary number of binding sites. Each binding site represents an energy minimum, corresponding in all likelihood to a fixed negative charge. Only one ion, at most, is allowed in the channel in the low occupancy case, as schematically illustrated by the circle in the second energy well from the left. Only one vacancy, at most, is allowed in the single vacancy case, which is schematically illustrated in B. The barriers to ion motion within the channel in B are considerably less than in A. The reason for this is that the 'movement' of the vacancy in this model cannot be rate limiting (Kohler & Heckmann, 1979). Further details of these models can be found in Hille & Schwarz (1978) and Schumaker & Mackinnon (1990).

distances (d_1 and d_2) of the barriers in Fig. 4 A, as indicated in the inset of Fig. 3 with $d_1 = 0.08$ and $d_2 = 0.17$. The solution to the model can be written down in analytical form for this case, although a numerical solution is more convenient in general, as illustrated in the Appendix. The fit of the model for these conditions is shown in Fig. 3 by the dashed lines labelled b.

Effect of ion concentration on conductance

The theory underlying eqn (2) (and also the GHK equation) is based on the independence principle, that is, the assumption that ions move independently of one another as they cross the channel. One manifestation of this principle is that the slope conductance of the current–voltage relation at strongly negative potentials is a linear function of $[K^+]_o$, or, stated differently, the slope conductance at 0 mV under equimolar conditions is a linear function of the equimolar concentration. These results are shown in Fig. 5. The intra- and extracellular concentrations were changed in parallel in these experiments (Methods), and the conductance was measured following a pre-pulse to 0 mV. The conductance appears to be well

described by a straight line. This relation does ultimately become saturated, with $[K^+]_i = [K^+]_o > 1$ M, as shown by Waggoner & Oxford (1987).

Alternative descriptions of the current–voltage relation

The analysis presented so far is clearly at odds with the tracer flux ratio results of Hodgkin & Keynes (1955) and Begenisich & DeWeer (1980). On the one hand the
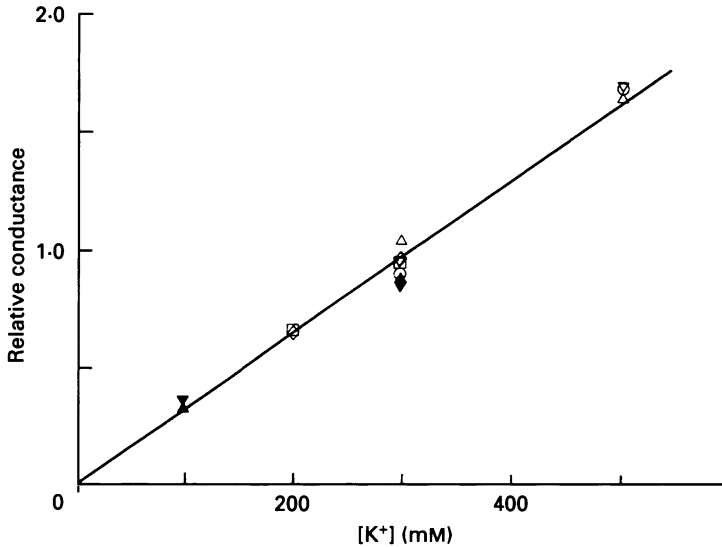

Fig. 5. Relationship between the conductance at 0 mV under equimolar potassium ion conditions $[K^+]_o = [K^+]_i$ as a function of the concentration. Each symbol represents a different axon. The experiments with 300 and 500 mM-K^+ ($\triangle$, ∇, $\bigcirc$) were obtained in 50 mM $[K^+]_o$ and 300 or 500 mM $[K^+]_i$. A 30 ms pre-pulse to -40 mV was used to slightly activate the conductance, followed by a test step to $+80$ mV.

current–voltage relations are consistent with the independence principle, whereas the tracer flux results are not. This paradox can be resolved by using a multiple-occupancy theory which gives current–voltage relations similar to the prediction of the GHK equation. One way to do this has been shown by Kohler & Heckmann (1979) and Schumaker & MacKinnon (1990) with the 'single vacancy' model illustrated in Fig. 4 *B*, in which one vacancy, at most, is allowed within the channel even with low ion activity conditions. The prediction of the model under these conditions for an arbitrary number of barriers (all barriers within the channel are identical and symmetric) is given by

$$J_K \cong \frac{(\exp(V'/m)-1)\,([K^+]_i\exp(V')-[K^+]_o)}{\cosh(V'/2m)\,(\exp(V')-\exp(V'/m))}, \tag{3}$$

where $\cosh(x) = (\exp(x)+\exp(-x))/2$ (see Appendix). In the limit $m \to \infty$, eqn (3) also takes on the voltage dependence of the GHK equation. The fit of eqn (3) to the data in Fig. 3 with $m = 4$ is not satisfactory (not shown). A much better fit can be

obtained, as in the low-occupancy model, by altering the position of the barriers so that each binding site adjacent to the central site is closer to its respective margin of the electric field ($d_1 = 0.08$; $d_2 = 0.17$, as before; inset of Fig. 6). Under these conditions, the fit to the data is almost equivalent to that of the GHK equation, as
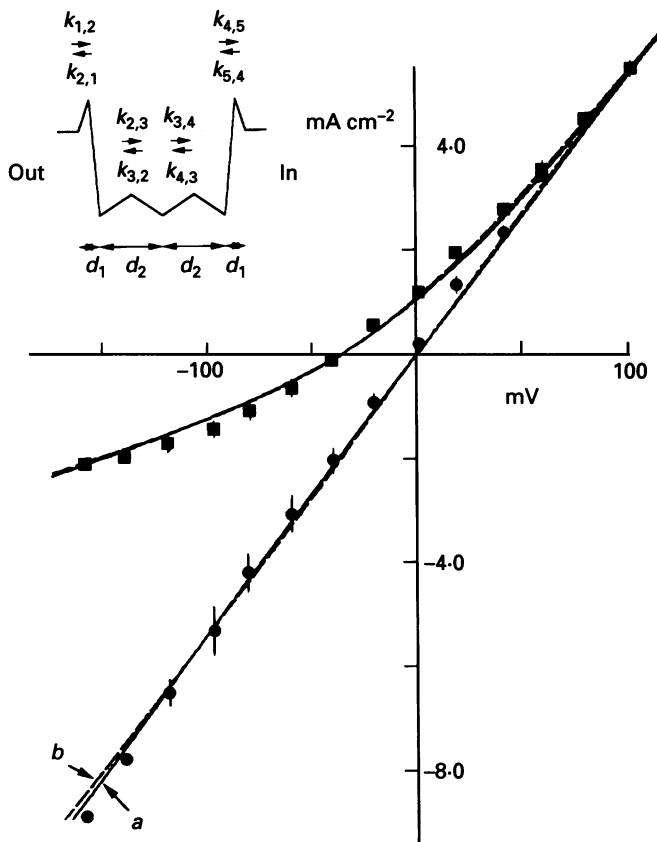

Fig. 6. Same data as in Fig. 3. The continuous lines represent the GHK equation, as in Fig. 3. The dashed lines (labelled b) represent the best fit to these results of the single vacancy model, eqn (5) in the text. The model is illustrated in the inset. The rate constants of the model are defined in the Appendix. ■, 50 mM $[K^+]_o$; ●, 300 mM $[K^+]_o$.

shown in Fig. 6 (dashed lines). The solution of the model for this case can be written in a compact form as

$$J_K \cong \frac{\exp\left(-(2d_1+d_2)V'\right)\left([K^+]_i \exp(V') - [K^+]_o\right)}{\cosh(d_1 V')\exp(3d_2 V') + 2\cosh(d_2 V')}, \tag{5}$$

with $d_1 = 0.07$ and $d_2 = 0.18$.

DISCUSSION

The current–voltage relation of the delayed rectifier current in squid axons has traditionally been characterized as a linear function of the driving force, $V - E_K$, regardless of the relative values of $[K^+]_o$ and $[K^+]_i$ based on the original observations

of Hodgkin & Huxley (1952*a*). The results in Fig. 3 demonstrate that this relation is a non-linear function of the driving force when the intra- and extracellular potassium ion concentrations differ. A similar result has recently been reported for squid giant axons by Kukita (1988). The discrepancy between these results and those of Hodgkin & Huxley (1952*a*) may be attributable to the smaller range of voltages (-90 to $+20$ mV) which they used. The non-linearity is more readily apparent when a broader voltage range is used, as in Fig. 3. The effect of a change in either bathing ion concentration on the *I–V* relation, which leads to the non-linearity when $[K^+]_o \neq [K^+]_i$, is significant, because it is consistent with the idea that the channel is occupied by only a single ion. The tracer flux results of Begenisich & DeWeer (1980) demonstrate that this conclusion cannot be correct. The results of Vestergaard-Bogind *et al.* (1985) are even more compelling in this regard, because they found a tracer flux ratio coefficient of ~ 2.7 for the Ca^{2+}-activated potassium channel in red blood cells for $[K^+]_o$ as low as 1 mM and $[K^+]_i$ as low as 30 mM. In other words, potassium channels appear to have a high degree of occupancy even in bathing media having low potassium ion activities. These observations are consistent with the 'single vacancy' model (Kohler & Heckmann, 1979; Schumaker & MacKinnon, 1990). A high ion turnover rate can be achieved in this scheme provided that the vacancy can rapidly move through the channel and that an ion can readily exit from the fully saturated state of the channel. Under these conditions, the model can give current–voltage relations which are very similar to the prediction of the GHK equation. That is, the resolution to the paradox suggested by the current–voltage relations and the tracer flux results is that the delayed rectifier channel may indeed obey the independence principle for ion *vacancies* rather than for ion *occupancies*.

The single-vacancy model predicts, by definition, a high tracer flux ratio exponent, n', in contrast to the low-occupancy model, which predicts $n' = 1$. The prediction of the single-vacancy model for a quadruple barrier, triple-binding site channel in the low ion strength regime is $n' = 3$, independent of $(V - E_K)$ (Schumaker & MacKinnon, 1990; see also Appendix), which is at least qualitatively consistent with the results of Benisich & DeWeer (1980). However, their results are consistent with a voltage dependence for n', which is not contained in the model. The results of Vestergaard-Bogind *et al.* (1985) show a lack of voltage dependence of n' ($n' = 2.7$) for a range of $V - E_K$ from -6 to $+90$ mV.

The primary conclusion of the analysis given above is that the description of the fully activated current–voltage relation for I_K in the Hodgkin & Huxley model (1952*b*) of ion currents in squid axons should be revised. This component is given by $g_K(V - E_K)$ in their model with the potassium conductance $g_K = 36$ mS cm^{-2}. Consequently, the fully activated current at 0 mV under physiological conditions ($[K^+]_o = 10$ mM) is ~ 2.5 mA cm^{-2}, which is within the range of measurements of I_K in these experiments. A more realistic description of I_K is provided by

$$\bar{I}_K = qN_K J_K = qN_K \frac{a \exp\left(-(2d_1 + d_2)qV/kT\right)\left([K^+]_i \exp\left(qV/kT\right) - [K^+]_o\right)}{2\cosh\left(d_1 qV/kT\right)\left(\exp\left(3d_2 qV/kT\right) + 2\cosh\left(d_2 qV/kT\right)\right)}, \quad (6)$$

where q is the unit electronic charge, N_K is the channel density, which is approximately 60 μm^{-2} based on noise measurements (Conti, DeFelice & Wanke, 1975), k is the Boltzmann constant, $d_1 = 0.07$, $d_2 = 0.18$, and a is the probability for

an ion from either side of the membrane to move into a vacancy in the channel (Appendix). To give a current amplitude of 2.5 mA cm^{-2} at 0 mV under physiological conditions, this parameter would be equal to 5.3×10^7 M^{-1} s^{-1}.

Current–voltage relations which are consistent with the GHK equation have been reported for potassium channels in various preparations beginning with the original observation of this result for the delayed rectifier in frog node of Ranvier by Frankenhaeuser (1962), and the delayed rectifier from the giant axon of *Myxicola* (Binstock & Goldman, 1971); the serotonin-sensitive channel in *Aplysia* sensory neurons (Siegelbaum, Camardo & Kandel, 1982); and delayed rectifiers from jellyfish axons (Mackie & Meech, 1989). However, the GHK equation does not appear to apply for the large-conductance, Ca^{2+}-activated potassium channels, given that the conductance of these channels becomes saturated for potassium ion concentrations of 200–300 mM (Latorre & Miller, 1983). The latter authors, and also Blatz & Magleby (1984), have shown that the activity–conductance relation for the Ca^{2+}-activated potassium channel can be described by a single-binding site model, a conclusion which is at odds with the results of Vestergaard-Bogind *et al.* (1985) and Neyton & Miller (1988). This difference in interpretation can be readily resolved by the single-vacancy model, as illustrated by Schumaker & MacKinnon (1990). Saturation of conductance occurs in this model when the exit of an ion from the fully saturated state is the rate-limiting step. This occurs when the ion activities in the bathing media are sufficiently large so that the probability that the channel is in its fully saturated state is significant relative to the probability that the channel is in one of its single-vacancy states.

The only potassium channel preparations for which tracer flux ratio results have been reported are those of the delayed rectifiers in cuttlefish and squid giant axons (Hodgkin & Keynes, 1955; Begenisich & DeWeer, 1980), the inward rectifier in frog skeletal muscle (Horowicz, Gage & Eisenberg, 1968), which has a current–voltage relation which also is not consistent with the GHK equation, and the Ca^{2+}-activated potassium channel in red blood cells (Vestergaard-Bogind *et al.* 1985). All of these results are consistent with a tracer flux ratio exponent of 2–3, which suggests that multiple occupancy is a general feature of potassium channels, including those which have current–voltage relations which are consistent with the GHK equation. The analysis in this study provides a self-consistent description of ion permeation for those kinds of potassium channels, a theory which is consistent with both the current–voltage relations and the tracer flux ratio results.

APPENDIX

The net flux for the barrier profile in Fig. $4A$ in the low-occupancy limit is given by

$$J = \exp(\nu)\,([K^+]_i \exp(V') - [K^+]_o)/(1 + \exp(2\nu) + \exp(4\nu) + \exp(6\nu) + \ldots),$$

$$= \exp(-\nu)\,([K^+]_i \exp(V') - [K^+]_o)/\sum_{j=0}^{m-1} = \exp(2j\nu), \qquad (A\,1)$$

as can be shown by induction from eqn (2) in Hille (1975), where m is the number of barriers, $\nu = V'/(2m)$, and $V' = qV(kT)$. The denominator in eqn (A 1) can be

summed exactly to give eqn (2) in the text. The solution to the model is more complicated when the electrical distances of the barriers are not all the same, as in the inset of Fig. 3. The flux can be numerically solved by inverting the matrix of coefficients for the equations which determine the probabilities, p_i, that the channel is in one of its four states. These are the probability that the channel is in its unoccupied state, p_1; the state with an ion in the outermost site of the channel, p_2; an ion in the central site, p_3; and an ion in the innermost site, p_4, respectively. The equations for these four quantities are

$$0 = k_{2,1}p_2 + k_{4,3}p_4 - (k_{1,2} + k_{5,4})p_1, \tag{A 2}$$

$$0 = k_{1,2}p_1 + k_{3,2}p_3 - (k_{2,1} + k_{2,3})p_2 \tag{A 3}$$

and

$$0 = k_{2,3}p_2 + k_{4,3}p_4 - (k_{3,2} + k_{3,4})p_3, \tag{A 4}$$

with $p_1 + p_2 + p_3 + p_4 = 1$ and $k_{1,2} = Q[K^+]_o \exp(-d_1 V')$, $k_{2,3} = \gamma \exp(-d_2 V')$, $k_{3,4} = \gamma \exp(-d_2 V')$, $k_{4,5} = \gamma \exp(-d_1 V')$, $k_{5,4} = Q[K^+]_i \exp(d_1 V')$, $k_{4,3} = \gamma \exp(d_2 V')$, $k_{3,2} = \gamma \exp(d_2 V')$, and $k_{2,1} = \gamma \exp(d_1 V')$, where Q and γ are frequency factors. The net flux, J, is given by the net flux across any barrier. For example, $J = k_{4,3}p_4 - k_{3,4}p_3$. The equations for p_i were solved using the Crout (1941) variation of the Gaussian elimination procedure. The result of this calculation is given by the dashed line (labelled b) in Fig. 3.

The net flux for the 'single vacancy' model illustrated in Fig. 4B is given by (Schumaker & MacKinnon, 1990)

$$J = D^{-1}([K^+]_i \exp(V'/2) - [K^+]_o \exp(-V'/2)) \tag{A 5}$$

where D is given by $\exp(V'/2)(\exp(V'/m) - 1)/(\cosh(V'/2m)\exp(V') - \exp(V'/m))$ when all terms containing concentration dependence are deleted (eqn (3) in the text). The prediction of the model for the barrier profile shown in the inset of Fig. 6 was obtained by solving the set of algebraic equations for the probabilities, p_i, that the channel is in one of its four states. These are the probability that the channel is in its fully saturated state, p_1; in the state with the innermost site vacant, p_2; in the state with central site vacant, p_3; and in the state with the outermost site vacant, p_4. These quantities are the solutions to the following equations,

$$0 = k_{1,2}p_2 + k_{3,4}p_4 - (k_{2,1} + k_{4,5})p_1, \tag{A 6}$$

$$0 = k_{2,1}p_1 + k_{2,3}p_3 - (k_{1,2} + k_{3,2})p_2 \tag{A 7}$$

$$0 = k_{3,2}p_2 + k_{3,4}p_4 - (k_{2,3} + k_{4,3})p_3, \tag{A 8}$$

and $1 = p_1 + p_2 + p_3 + p_4$, where $k_{2,3} = k_{3,4} = \gamma \exp(-d_2 V')$, $k_{4,3} = k_{3,2} = \gamma \exp(d_2 V')$, $k_{1,2} = a[K^+]_o \exp(-d_1 V')$, $k_{5,4} = a[K^+]_i \exp(d_1 V')$, $k_{2,1} = b \exp(d_1 V')$, and $k_{4,5} = b \exp(-d_1 V')$, where a and b are constants. The symmetry between the single-vacancy model and the single-occupancy model is apparent from a comparison of eqns (A 1) to (A 3) with eqns (A 6) to (A 8). The net flux is equal to $J = k_{4,3}p_3 - k_{3,4}p_2$. The analytical solution for this case is given in eqn (5) in the text.

The tracer fluxes were calculated by assuming that all ions on one side were labelled. The model has twelve states in this case. The matrix of coefficients for the

probabilities was inverted with the Crout (1941) version of the Gaussian elimination procedure.

REFERENCES

BEGENISICH, T. & DEWEER, P. (1980). Potassium flux ratio in voltage-clamped squid giant axons. *Journal of General Physiology* **76**, 83–93.

BINSTOCK, L. & GOLDMAN, L. (1971). Rectification in instantaneous potassium current–voltage relations in *Myxicola* giant axons. *Journal of Physiology* **217**, 517–531.

BLATZ, A. L. & MAGLEBY, K. L. (1984). Ion conductance and selectivity of single calcium-activated potassium channels in cultured rat muscle. *Journal of General Physiology* **84**, 1–23.

CLAY, J. R. (1984). Potassium channel kinetics in squid axons with elevated levels of external potassium concentration. *Biophysical Journal* **45**, 481–485.

CLAY, J. R. & SHLESINGER, M. F. (1983). Effects of external cesium and rubidium on outward potassium currents in squid axons. *Biophysical Journal* **42**, 43–53.

CONTI, F., DEFELICE, L. J. & WANKE, E. (1975). Potassium and sodium ion current noise in the membrane of the squid giant axon. *Journal of Physiology* **248**, 45–82.

CROUT, P. D. (1941). A short method for evaluating determinants and solving systems of linear equations with real or complex coefficients. *Transactions of the American Institute of Electrical Engineers* **60**, 1235–1241.

FRANKENHAEUSER, B. (1962). Potassium permeability in myelinated nerve fibres of *Xenopus laevis*. *Journal of Physiology* **160**, 54–61.

GLASSTONE, S., LAIDLER, K. J. & EYRING, H. (1941). *The Theory of Rate Processes*. McGraw–Hill Book Company, New York.

GOLDMAN, D. E. (1943). Potential, impedance, and rectification in membranes. *Journal of General Physiology* **27**, 37–60.

HILLE, B. (1975). Ionic selectivity, saturation, and block in sodium channels. A four-barrier model. *Journal of General Physiology* **66**, 535–560.

HILLE, B. & SCHWARZ, W. (1978). Potassium channels as multi-ion single-file pores. *Journal of General Physiology* **72**, 409–442.

HODGKIN, A. L. & HUXLEY, A. F. (1952a). Currents carried by sodium and potassium ions through the membrane of the giant axon of *Loligo*. *Journal of Physiology* **116**, 449–472.

HODGKIN, A. L. & HUXLEY, A. F. (1952b). A quantitative description of membrane current and its application to conduction and excitation in nerve. *Journal of Physiology* **117**, 500–544.

HODGKIN, A. L. & KATZ, B. (1949). The effect of sodium ions on the electrical activity of the giant axon of the squid. *Journal of Physiology* **108**, 37–77.

HODGKIN, A. L. & KEYNES, R. D. (1955). The potassium permeability of a giant nerve fibre. *Journal of Physiology* **128**, 61–88.

HOROWICZ, P., GAGE, P. W. & EISENBERG, R. S. (1968). The role of the electrochemical gradient in determining potassium fluxes from striated muscle. *Journal of General Physiology* **51**, 193–203s.

KOHLER, H.-H. & HECKMANN, K. (1979). Unidirectional fluxes in saturated single file pores of biological and artificial membranes. I. Pores containing no more than one vacancy. *Journal of Theoretical Biology* **79**, 381–401.

KUKITA, F. (1988). Removal of periaxonal potassium accumulation in a squid giant axon by outward osmotic water flow. *Journal of Physiology* **399**, 647–656.

LATORRE, R. & MILLER, C. (1983). Conduction and selectivity in K+ channels. *Journal of Membrane Biology* **71**, 11–30.

MACKIE, G. O. & MEECH, R. W. (1989). Potassium channel family in axons of the jellyfish *Aglantha digitale*. *Journal of Physiology* **418**, 14P.

NEYTON, J. & MILLER, C. (1988). Discrete Ba^{2+} block as a probe of ion occupancy and pore structure in the high-conductance Ca^{2+} activated K+ channel. *Journal of General Physiology* **92**, 569–586.

SCHUMAKER, M. F. & MACKINNON, R. (1990). A simple model for multi-ion permeation. Single-vacancy conduction in a simple pore model. *Biophysical Journal* **58**, 975–984.

SIEGELBAUM, S. A., CAMARDO, J. S. & KANDEL, E. R. (1982). Serotonin and cAMP close single K channels in *Aplysia* sensory neurones. *Nature* **299**, 413–417.

SWENSON, R. P. & ARMSTRONG, C. M. (1981). K^+ channels close more slowly in the presence of external K^+ and Rb^+. *Nature* **291**, 427–429.

VESTERGAARD-BOGIND, B., STAMPE, P. & CHRISTOPHERSEN, P. (1985). Single-file diffusion through the Ca^{2+} activated K^+ channel of human red blood cells. *Journal of Membrane Biology* **88**, 67–75.

WAGGONER, P. K. & OXFORD, G. S. (1987). Cation permeation through the voltage-dependent potassium channel in the squid axon. Characteristics and mechanisms. *Journal of General Physiology* **90**, 261–290.